ELSEVIER

Contents lists available at ScienceDirect

# Catalysis Communications

journal homepage: www.elsevier.com/locate/catcom

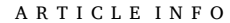


### Short communication

# Crystal size sensitivity of HMOR zeolite in dimethyl ether carbonylation

Fuli Wen a,b,c,1, Xiangnong Ding a,b,c,1, XuDong Fang a,b,c, Hongchao Liu a,b,\*, Wenliang Zhu a,b,\*

- <sup>a</sup> National Engineering Laboratory for Methanol to Olefins, Dalian Institute of Chemical Physics, Chinese Academy of Sciences, Dalian 116023, China
- b Dalian National Laboratory for Clean Energy, Dalian Institute of Chemical Physics, Chinese Academy of Sciences, Dalian 116023, China
- <sup>c</sup> University of Chinese Academy of Sciences, Beijing 100049, China



Keywords: H-mordenite Crystal size Dimethyl ether Carbonylation Diffusion

#### ABSTRACT

The effect of crystal size of HMOR from micro size to 50 nm, with the apparent similar acid site density, on catalytic performance for the dimethyl ether (DME) carbonylation was investigated. The crystal size of HMOR is sensitive to the deactivation rate of DME carbonylation reaction, and the higher stability around 200 nm can be achieved. The characterization studies reveal that the diffusions of MA product play a key role during the induction and deactivation period in DME carbonylation. These will be helpful for guiding the large-scale synthesis of mordenite zeolites catalysts with high efficiencies for DME carbonylation.

### 1. Introduction

Ethanol has gained tremendous interest since it can be used as fuels, fuel additive, chemical feedstock, and so on [1]. Up to now, the conventional grain-based fermentation is still the commercial route for ethanol production round the world. Unfortunately, this is not suitable for China based on the consideration of food security of 1.4 billion people [2]. Thus, it is necessary and urgent to develop an alternative ethanol production route from other resources. Recently, the selective carbonylation of dimethyl ether (DME) to methyl acetate (MA) on solid zeolites followed by hydrogenation of MA over the copper-based catalysts, has attracted great attention due to its high atom economy and environmental friendliness [3-7]. More interestingly, DME as a "circular hydrogen carrier" if it is generated from CO2 and H2 from renewable can provide H<sub>2</sub> for hydrogenation of MA to ethanol [8]. However, low activity and stability of zeolites in the carbonylation reaction is challenging, therefore, numerous studies have been conducted to seek highly efficient catalysts of DME carbonylation for industrial practices.

Up to now, HMOR zeolite has been found to be the most active catalyst in DME carbonylation among the zeolites with different topologies [3,9]. MOR is characterized by a channel system composed of 12-membered ring (MR) main channel (0.65  $\times$  0.7 nm) and 8-MR channel (0.26  $\times$  0.57 nm) in the crystallographic c direction, which are connected to an 8-MR side pocket along the b direction [10]. Experimental and theoretical analyses have revealed that the acid sites within 8-MR

channels of HMOR are the active centers for DME carbonylation [11–13]. Unfortunately, HMOR suffers from fast deactivation due to coke produced from DME in 12-MR [14], which prevents the occurrence of carbonylation reaction in 8-MR channels [11,15]. Therefore, it is urgent and challenging to decrease or eliminate the formation of coke in 12-MR channels and thus improve catalytic activity and stability of HMOR zeolite during DME carbonylation.

Reducing the crystal size of zeolite is an effective method to improve their catalytic performance in many reactions [16-19]. Regarding the process of DME carbonylation, there are three stags including induction, stable and deactivation periods. Different nanosized-mordenites have also been employed in this process and their effect on the stable and deactivation periods are often focused. [20-24]. Mordenite nanosheets with different thickness were fabricated, and exhibited the higher catalytic activity and stability than the commercial zeolites, which proves that the strategy of controlling crystal orientation during the hydrothermal synthesis reaction is an effective approach to promote the performance of HMOR zeolite [21,22]. Further, a series of rod-assembled HMOR were successfully synthesized with a controllable c/b ratio. MA formation rates increase with enhancing c/b ratio whereas the catalysts suffer from the faster deactivation [23]. Our group has also successfully prepared a nanocrystal-assembled HMOR zeolite with 20-50 nm crystallites and achieved the higher activity and stability than micro-sized MOR zeolite in the DME carbonylation [24]. Induction period is an initial stage which relate to initial organic compounds formation on the

<sup>\*</sup> Corresponding authors at: National Engineering Laboratory for Methanol to Olefins, Dalian Institute of Chemical Physics, Chinese Academy of Sciences, Dalian 116023, China.

E-mail addresses: chliu@dicp.ac.cn (H. Liu), wlzhu@dicp.ac.cn (W. Zhu).

 $<sup>^{1}\,</sup>$  The authors contributed equally to this work.

surface of HMOR in DME carbonylation reaction [13]. Unfortunately, the effect of different parameters on the induction period is hardly mentioned. On the other hand, the smaller crystal sizes must result in the higher costs of synthesis and separation, indicating that seeking MOR zeolite with suitable crystal size, eligible catalytic performance to meet the needs of industrial production but low synthesis cost, is of great significance for commercialization of this new approach for ethanol production. Thus, from viewpoint of industrial practices, it is desirable to establish a crystal size-reactivity relationship to guide the synthesis of MOR zeolites in large-scale.

Herein, HMOR zeolites from 9  $\mu m$  to around 50 nm with the similar Si/Al ratios were employed as catalysts in the DME carbonylation. The relationships between the adsorption capability, diffusion property and reaction behavior of HMOR with different sizes of crystal were investigated. It was found that the crystal size between 330 and 200 nm is quite sensitive to the DME carbonylation reaction. The induction periods become longer with reducing crystal size below 330 nm. The higher stability of HMOR catalyst is obtained when the crystal size is around 200 nm, which is helpful to guide the production of industrial zeolites catalyst. Moreover, the diffusion of MA within the HMOR zeolite plays an important role in determining the lifetime of HMOR catalyst in DME carbonylation reaction.

### 2. Experimental

#### 2.1. Materials and methods

HMOR zeolites were obtained through ion-exchange methods, the details information of samples and preparation methods were given in ESI. The samples with crystal size increased were named as HMOR-1, HMOR-2, HMOR-3. The nanocrystal-assembled HMOR zeolite composed of 20–50 nm was used as a reference catalyst, named as HMOR-R [24].

### 2.2. Characterization

XRD patterns of the samples were recorded on PANalytical X'Pert PRO X-ray diffractometer. The relative crystallinity was determined from the peak intensity using HMOR-1 sample as reference. XRF analysis was performed on Philips Magix X-ray fluorescence spectrometer. FESEM images were taken with a Hitachi SU8020 microscope at 2.0 kV accelerating voltage. N2 adsorption-desorption experiments were performed at 77 K on a Micromeritic ASAP 2020 instrument. NH3-TPD analysis was were recorded on Micromeritics AutoChem II 2920. FT-IR analysis using D<sub>3</sub>-acetonitrile as a probe molecule were recorded with a Bruker Tensor 27 FT-IR spectrometer according to the literature [25]. TG were performed on the automatic TG/DTA instrument. Solid-state NMR spectra were obtained on a Bruker Avance III 600 MHz spectrometer with a 4 mm MAS probe. The uptake rate and adsorption isotherm were measured on an Intelligent Gravimetric Analyzer (IGA-100, Hidden Analytical). The details of characterization experiments could be found in ESI.

### 2.3. Catalyst evaluation

The reaction of DME carbonylation was tested in a continuous flow stainless steel fixed-bed reactor at 473 K, 2.0 MPa. The details of experiments could be found in ESI.

# 3. Results and discussion

# 3.1. Textural and chemical properties of the catalysts

SEM images (Fig. S1) illustrate that three samples possess similar plate-like assembled structures. By measuring through SEM, the crystal sizes of HMOR-1 and HMOR-2 are about 200 nm and 330 nm,

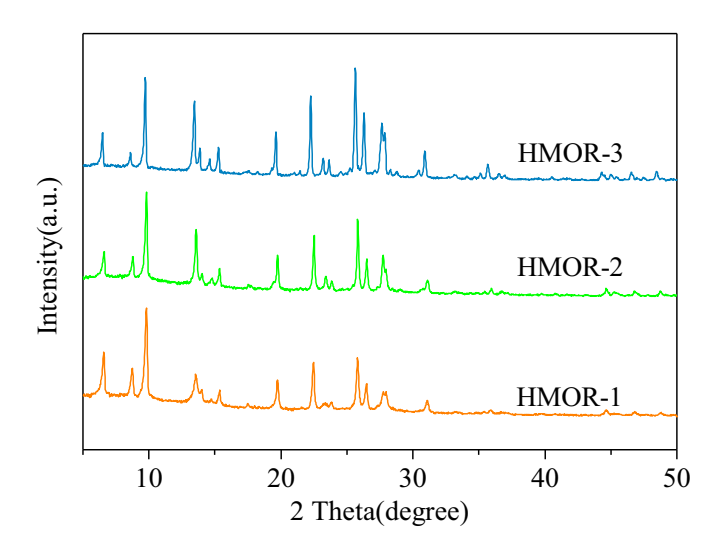


Fig. 1. XRD patterns of the HMOR-x catalysts.

respectively, whereas the HMOR-3 is a micro-sized material with a size of about 9 µm. The powder XRD patterns of samples as shown in Fig. 1, all the samples exhibit a pure HMOR phase with good crystallinity. The diffraction peaks of the HMOR-1 sample are much broader compared to the other two HMOR zeolites, indicating that HMOR-1 has a smaller crystal size, which is consistent with the results obtained from SEM images. The N<sub>2</sub> physisorption isotherms of the three as-prepared HMOR zeolites are displayed in Fig. S2, which can be considered as the combination of type I plus type IV isotherm. These observations are suggesting the coexistence of mesoporous and microporous. However, only hysteresis loops are observed in the relatively high pressure, indicating that most mesoporous likely result from the stacking spaces of crystal. The detailed textural properties are listed in Table 1. The BET and external surface areas, micropore surface area and micropore volume all increase as the crystal size decreases, which is consistent with the increase in specific surface area as the particle size decreases. The Si/Al ratios of the three samples are 8.31, 8.44, and 8.44, respectively, implying that all as-prepared HMOR zeolites have similar Si/Al ratios.

Fig. S3a displays the NH<sub>3</sub>-TPD profiles of HMOR samples. Two ammonia desorption peaks at lower temperatures of around 220 °C and higher temperatures of about 520  $^{\circ}$ C, corresponding to the weak and strong acid sites [26], respectively, can be observed obviously. The positions of higher temperature ammonia desorption peak are almost the same, although the crystal sizes are different, indicating that acid strength of different samples are apparently similar. Moreover, the <sup>1</sup>H NMR spectrum was performed to quantify the total amount of Brønsted acid sites for the catalysts. As shown in Fig. S3b, the samples show three bands at 1.8 ppm, 2.2 ppm and 3.8 ppm in the range of 1-6 ppm, representing the terminal silanol groups, the extra-framework aluminum species, and the bridged hydroxyl (Si-OH-Al), respectively [27]. The signal intensity at 3.8 ppm of these samples is highly similar, corroborating with the results of the NH<sub>3</sub>-TPD. In order to strictly quantify the Brønsted acid sites, deconvolution analysis of the spectrum was carried out and the detailed results are listed in Table 1. The Brønsted acid densities of samples are 1.14, 1.27 and 1.15 mmol/gcat, respectively, for the HMOR-1, HMOR-2, and HMOR-3. These suggest that the dramatic discrepancies in acid properties could be excluded despite their difference in crystal size.

## 3.2. DME carbonylation

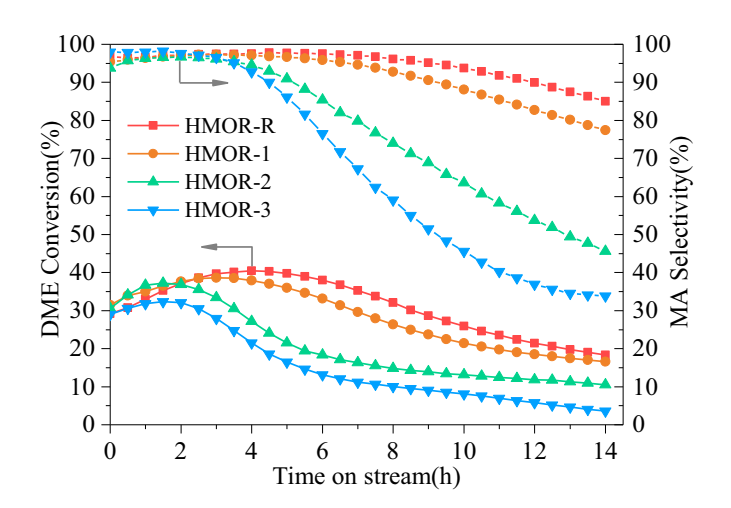
The catalytic performance of the samples was carried in a fixed-bed reactor at 473 K, 2.09 MPa, and GHSV of 1500 ml/g·h. The DME conversion and product selectivity versus time on stream are illustrated in

Table 1
Composition, Brønsted acid density and Textural Properties of HMOR with Different Crystal Sizes.

Sample	Si/Al <sup>a</sup>	Acid density <sup>b</sup> (mmol/g)	Relative crystallinity <sup>c</sup> (%)	Surface area (m <sup>2</sup> /g)			Pore volume (m <sup>3</sup> /g)	
				BET	Micropore	External	Total	Micropore
HMOR-R <sup>d</sup>	9.1	-	_	471	369	102	0.62	0.17
HMOR-1	8.31	1.14	100	472.7	417.8	55.0	0.26	0.19
HMOR-2	8.44	1.27	87	439.8	396.4	43.5	0.23	0.18
HMOR-3	8.44	1.15	101	322.8	290.0	32.8	0.17	0.13

<sup>&</sup>lt;sup>a</sup> Obtained from XRF results.

d data from reference [24].



**Fig. 2.** The DME conversion and MA selectivity of DME carbonylation over HMOR-x catalysts. Reaction conditions: T=473 K, P=2.09 MPa, DME/CO/N<sub>2</sub> = 5/35/60, GHSV = 1500 ml/g·h.

Fig. 2. The induction periods of 4, 3, 1.5 and 1.5 h were observed for HMOR-R, HMOR-1, HMOR-2 and HOMR-3, respectively, indicating that the crystal sizes in the special ranges would play an important role in the initial stage of DME carbonylation. Similar results could be found using HMOR nanosheet assemblies and nanocrystal-assembled hierarchical HMOR as catalysts, respectively, comparing with commercial microsized HMOR [22,24]. Compared with different samples, the DME conversion was obtained with 32.5% for the HMOR-3 zeolite with a crystal size of around 9 μm. Enhanced performance by smaller crystal sizes was

achieved with the DME conversions of 37.5%, 39.0% and 41.5% for the HMOR-2, HMOR-1 and HMOR-R, respectively. After the stable period, the catalysts begin to deactivate with the formations of hydrocarbons and methanol as the main byproducts in Fig. S5. The lower selectivities of byproducts could be achieved for the HMOR with shorter crystal size under the same reaction conditions, indicating that diffusion effect result from the changes of crystal size plays an important role in determining catalytic activities [20,24]. Moreover, the spent catalysts were investigated by TG/DTA analysis in Fig. S6. The peaks at about 320 °C and 600 °C could be observed, which are attributed from the adsorbed species such as the methyl and acetyl groups retained within the zeolite and the heavy coke species formed in the reaction process, respectively. For comparison, the lowest amount of coke species over HMOR-1 is achieved in the samples investigated. These suggest that the diffusion effect on carbonaceous deposits of HMOR-1 is strengthened due to the reduction of crystal size.

It has been accepted that the better stability of nano-sized catalysts can be obtained compared with that the micro-sized zeolite [20–22]. To determine the influence of the crystal size on the deactivation period, the deactivation rate constants from DME carbonylation were calculated by introducing the definition of deactivation degree  $(D_x)$  according to the literature [28]. The calculation formula of  $D_x$  is shown in Eq. (1):

$$D_{x} = \frac{STY_{MA}^{max} - STY_{MA}}{STY_{MA}^{max}} *100\%$$
 (1)

 $STY_{MA}^{max}$  is the maximum space time yield (STY) of MA during an experiment and  $STY_{MA}$  is the STY at a given time after  $STY_{MA}^{max}$  has been reached. The plots of  $D_x$  as a function of the deactivation time are shown in Fig. 3a. It is evident that the linear relationship between the  $D_x$  and deactivation time, suggesting that the catalysts deactivate at a constant rate which can be represented using the slope of line. The deactivation rate values are 7.77, 8.47, 16.98 and 19.21% per hour for HMOR-R,

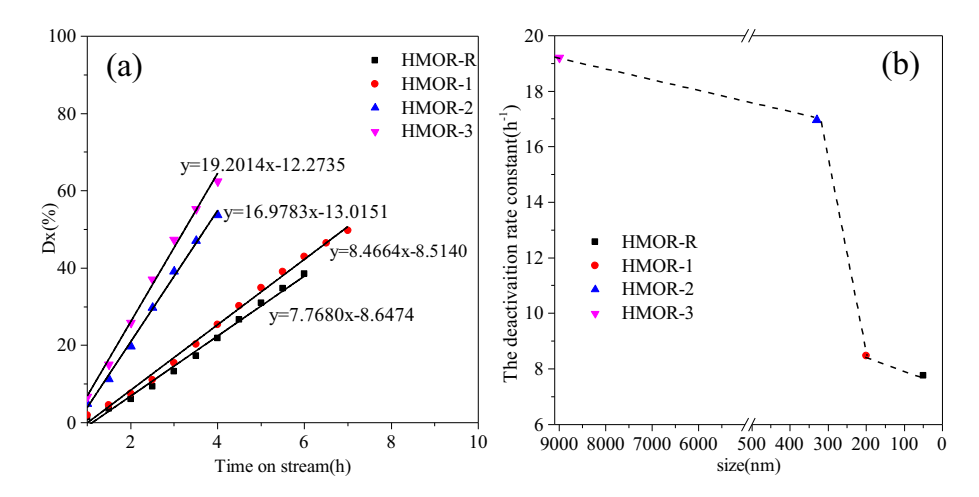


Fig. 3. (a) The degree of inactivation varies with time on stream over HMOR-1, HMOR-2 and HMOR-3; (b) The deactivation rate constant varies with the crystal size of HMOR zeolite.

<sup>&</sup>lt;sup>b</sup> Calculated from <sup>1</sup>H MAS NMR based on peak deconvolution.

<sup>&</sup>lt;sup>c</sup> Calculated based on the intensity of the eight strongest peaks( $2\theta = 6.544, 9.77, 13.53, 19.71, 22.43, 25.78, 26.44 and 27.79°) in the XRD patterns.$ 

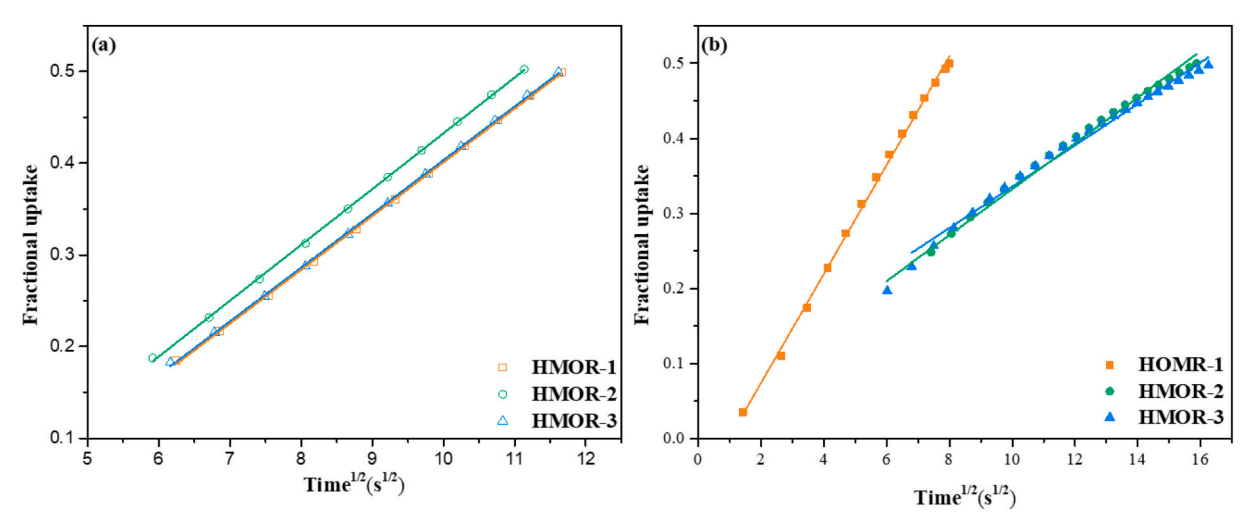


Fig. 4. Uptake rate for DME (a) and MA (b) in the HMOR-x zeolites at 313 K, respectively.

HMOR-1, HMOR-2 and HMOR-3, respectively. A plot of deactivation rates as functions of crystal size is shown in Fig. 3b. It is fascinating and unexpected that there is an inflection point between the deactivation rate and the crystal size. The deactivation rate reduced slightly when the crystal size is reduced from micron meter to around 330 nm. However, the dramatic change for the deactivation rate could be found when the crystal size is changed from 330 nm to 200 nm. The results indicate a critical value for crystal size on the stability of HMOR zeolites in the DME carbonylation.

### 3.3. Adsorption isotherm and uptake rate

It is widely accepted that the shortening of crystal size would enhance the diffusion of guest molecules in microporous zeolites [29-31]. Herein, the CO, DME, and MA, the reactant and product molecules, were employed as probe molecules to measure the adsorption behavior of HMOR with different crystal sizes by using IGA. Fig. S4 displays the adsorption isotherms with pressure for CO, DME and MA on the HMOR with different crystal sizes. The isotherms for DME and MA over the HMOR zeolites exhibit the typical Langmuir Type-I adsorption, which reach saturation at lower pressure and the increases slightly with further increase of pressure. However, the isotherms for CO showed a completely different trend compared to DME and MA on the HMOR with different crystal sizes. Furtherly, it can be observed that the saturated adsorption capacity increases with decreasing crystal size for the HMOR zeolites for all the probe molecules, especially for CO, which might be attributed to the changes of texture properties due to the reduction of crystal size considering the identical acidity properties [32]. Since it has been reported that the productivities of MA do increase linearly with CO pressure [3], we deduce that the increase of adsorption capability for CO might be responsible for the enhanced performance for HMOR with smaller crystal size. Moreover, the diffusivities of DME and MA except CO since its adsorption processes is fast equilibrium were measured under fixed certain pressure by uptake rate method. The effective diffusion coefficient was obtained by Fick's second law using Eq. (2) to fit the experimental results [33].

$$\frac{m(t)}{m(\infty)} = \frac{6}{\pi} \sqrt{\frac{D}{r^2}} \sqrt{t}$$
 (2)

Where m (t)/m ( $\infty$ ) represents the adsorption amount after normalization and r is the effective radius of crystal. The normalized loading varies with the  $t^{1/2}$  as shown in Fig. 4, and a linear relationship could be observed. The slopes of the curves represent the effective diffusion coefficients. The effective diffusion coefficients for DME in the HMOR-1, HMOR-2 and HMOR-3 are almost the same despite

remarkable difference in their crystal sizes (200 nm vs. 9  $\mu$ m). A remarkable difference of the slopes in the HMOR-1 and HMOR-2 could be found for the uptake rates for MA, whereas highly similar slopes can be obtained for HMOR-2 and HMOR-3. These results are consistent with their comparison in induction period and deactivation rate constants with crystal size in DME carbonylation [20]. Therefore, we can deduce that there is a "turning point" in the crystal size and the diffusion of MA play a critical role in the deactivation period for DME carbonylation.

### 4. Conclusions

In summary, the dependence of catalytic performances including induction, stable and deactivation periods on the crystal size of HMOR, with the similar acid properties, from micro-size to nano-size has been established. The enhancement of the adsorption capability of CO, due to the smaller crystal sizes of HMOR zeolite, results in the increase of activities for DME carbonylation. The induction and deactivation period in the DME carbonylation reaction is closely related to the diffusion of MA within the HMOR zeolites, and the longer induction period and slower deactivation rate can be achieved by enhancing the diffusion of MA. In addition, we proved that there is a certain "turning point" of crystal size between 200 and 330 nm, and the better stability can be obtained if the crystal size is about 200 nm. These results are helpful for development of industrial catalysts with high-efficiencies for ethanol synthesis via DME carbonylation route.

### **Declaration of Competing Interest**

Authors declare no conflict of interest.

### Acknowledgements

We acknowledge the financial support from the National Natural Science Foundation of China (Grant No. 21972141, 21991090 and 21991094), and the "Transformational Technologies for Clean Energy and Demonstration", Strategic Priority Research Program of the Chinese Academy of Sciences (Grant No. XDA21030100).

## Appendix A. Supplementary data

Supplementary data to this article can be found online at  $\frac{https:}{doi.}$  org/10.1016/j.catcom.2021.106309.

#### References

- [1] J. Goldemberg, Ethanol for a sustainable energy future, Science 315 (2007)
- [2] H. Wang, Z. Wu, Z. Tai, R. Pei, X. Ren, Advances in synthesis of anhydrous ethanol from syngas via carbonylation of dimethyl ether and hydrogenation of methyl acetate, Chem. Indust. Eng. Prog. 38 (2019) 4497–4503.
- [3] P. Cheung, A. Bhan, G.J. Sunley, E. Iglesia, Selective carbonylation of dimethyl ether to methyl acetate catalyzed by acidic zeolites, Angew. Chem. Int. Ed. 45 (2006) 1617–1620.
- [4] X.G. San, Y. Zhang, W.J. Shen, N. Tsubaki, New synthesis method of ethanol from dimethyl ether with a synergic effect between the zeolite catalyst and metallic catalyst, Energy Fuel 23 (2009) 2843–2844.
- [5] X.A. Li, X.G. San, Y. Zhang, T. Ichii, M. Meng, Y.S. Tan, N. Tsubaki, Direct synthesis of ethanol from dimethyl ether and syngas over combined H-Mordenite and cu/ ZnO catalysts, ChemSusChem 3 (2010) 1192–1199.
- [6] X.H. Gao, B.L. Xu, G.H. Yang, X.B. Feng, Y. Yoneyama, U. Taka, N. Tsubaki, Designing a novel dual bed reactor to realize efficient ethanol synthesis from dimethyl ether and syngas, Catal. Sci. Technol. 8 (2018) 2087–2097.
- [7] X.B. Feng, P.P. Zhang, Y. Fang, W. Charusiri, J. Yao, X.H. Gao, Q.H. Wei, P. Reubroycharoen, T. Vitidsant, Y. Yoneyama, G.H. Yang, N. Tsubaki, Designing a hierarchical nanosheet ZSM-35 zeolite to realize more efficient ethanol synthesis from dimethyl ether and syngas, Catal. Today 343 (2020) 206–214.
- [8] E. Catizzone, C. Freda, G. Braccio, F. Frusteri, G. Bonura, Dimethyl ether as circular hydrogen carrier: catalytic aspects of hydrogenation/dehydrogenation steps, J. Energy Chem. 58 (2021) 55–77.
- [9] E.S. Zhan, Z.P. Xiong, W.J. Shen, Dimethyl ether carbonylation over zeolites, J. Energy Chem. 36 (2019) 51-63.
- [10] W.M. Meier, The crystal structure of mordenite (ptilolite)\*, Zeitschrift für Kristallographie - Crystalline Materials 115 (1961) 439–450.
- [11] M. Boronat, C. Martinez-Sanchez, D. Law, A. Corma, Enzyme-like specificity in zeolites: a unique site position in Mordenite for selective Carbonylation of methanol and dimethyl ether with CO, J. Am. Chem. Soc. 130 (2008) 16316–16323.
- [12] A. Bhan, A.D. Allian, G.J. Sunley, D.J. Law, E. Iglesia, Specificity of sites within eight-membered ring zeolite channels for carbonylation of methyls to acetyls, J. Am. Chem. Soc. 129 (2007) 4919–4924.
- [13] P. Cheung, A. Bhan, G.J. Sunley, D.J. Law, E. Iglesia, Site requirements and elementary steps in dimethyl ether carbonylation catalyzed by acidic zeolites, J. Catal. 245 (2007) 110–123.
- [14] H. Zhou, W.L. Zhu, L. Shi, H.C. Liu, S.P. Liu, S.T. Xu, Y.M. Ni, Y. Liu, L. Li, Z.M. Liu, Promotion effect of Fe in mordenite zeolite on carbonylation of dimethyl ether to methyl acetate, Catal. Sci. Technol. 5 (2015) 1961–1968.
- [15] M. Boronat, C. Martinez, A. Corma, Mechanistic differences between methanol and dimethyl ether carbonylation in side pockets and large channels of mordenite, Phys. Chem. Chem. Phys. 13 (2011) 2603–2612.
- [16] L.H. Chen, X.Y. Li, J.C. Rooke, Y.H. Zhang, X.Y. Yang, Y. Tang, F.S. Xiao, B.L. Su, Hierarchically structured zeolites: synthesis, mass transport properties and applications, J. Mater. Chem. 22 (2012) 17381–17403.
- [17] Y.Y. Yuan, P. Tian, M. Yang, D. Fan, L.Y. Wang, S.T. Xu, C. Wang, D.H. Wang, Y. Yang, Z.M. Liu, Synthesis of hierarchical beta zeolite by using a bifunctional

- cationic polymer and the improved catalytic performance, RSC Adv. 5 (2015) 9852–9860.
- [18] E. Verheyen, C. Jo, M. Kurttepeli, G. Vanbutsele, E. Gobechiya, T.I. Korányi, S. Bals, G. Van Tendeloo, R. Ryoo, C.E.A. Kirschhock, J.A. Martens, Molecular shape-selectivity of MFI zeolite nanosheets in n-decane isomerization and hydrocracking, J. Catal. 300 (2013) 70–80.
- [19] M. Yang, P. Tian, C. Wang, Y.Y. Yuan, Y. Yang, S.T. Xu, Y.L. He, Z.M. Liu, A top-down approach to prepare silicoaluminophosphate molecular sieve nanocrystals with improved catalytic activity, Chem. Commun. 50 (2014) 1845–1847.
- [20] H.F. Xue, X.M. Huang, E. Ditzel, E.S. Zhan, M. Ma, W.J. Shen, Coking on micrometer- and nanometer-sized mordenite during dimethyl ether carbonylation to methyl acetate, Chin. J. Catal. 34 (2013) 1496–1503.
- [21] Y.H. Liu, N. Zhao, H. Xian, Q.P. Cheng, Y.S. Tan, N. Tsubaki, X.G. Li, Facilely synthesized H-Mordenite Nanosheet assembly for Carbonylation of dimethyl ether, ACS Appl. Mater. Interfaces 7 (2015) 8398–8403.
- [22] M. Ma, X.M. Huang, E.S. Zhan, Y. Zhou, H.F. Xue, W.J. Shen, Synthesis of mordenite nanosheets with shortened channel lengths and enhanced catalytic activity, J. Mater. Chem. A 5 (2017) 8887–8891.
- [23] Y. Li, Z.H. Li, S.Y. Huang, K. Cai, Z. Qu, J.F. Zhang, Y. Wang, X.B. Ma, Morphology-dependent catalytic performance of Mordenite in Carbonylation of dimethyl ether: enhanced activity with high c/b ratio, ACS Appl. Mater. Interfaces 11 (2019) 24000–24005.
- [24] Y.Y. Yuan, L.Y. Wang, H.C. Liu, P. Tian, M. Yang, S.T. Xu, Z.M. Liu, Facile preparation of nanocrystal-assembled hierarchical mordenite zeolites with remarkable catalytic performance, Chin. J. Catal. 36 (2015) 1910–1919.
- [25] E. Catizzone, M. Migliori, T. Mineva, S. van Daele, V. Valtchev, G. Giordano, New synthesis routes and catalytic applications of ferrierite crystals. Part 1: 1,8-Diaminooctane as a new OSDA, Microporous Mesoporous Mater. 296 (2020) 109987.
- [26] F. Lónyi, J. Valyon, On the interpretation of the NH3-TPD patterns of H-ZSM-5 and H-mordenite, Microporous Mesoporous Mater. 47 (2001) 293–301.
- [27] D. Freude, M. Hunger, H. Pfeifer, W. Schwieger, 1H MAS NMR studies on the acidity of zeolites, Chem. Phys. Lett. 128 (1986) 62–66.
- [28] D.B. Rasmussen, A.D. Jensen, J.M. Christensen, P.G. Moses, A. Riisager, J. Rossmeisl, F. Studt, P.A. Jensen, J. Sehested, O. Swang, B. Temel McKenna, Selective and Efficient Synthesis of Ethanol from Dimethyl Ether and Syngas, Technical University of Denmark, 2015.
- [29] A.A. Rownaghi, F. Rezaei, J. Hedlund, Selective formation of light olefin by n-hexane cracking over HZSM-5: influence of crystal size and acid sites of nano- and micrometer-sized crystals, Chem. Eng. J. 191 (2012) 528–533.
- [30] M. Guisnet, L. Costa, F.R. Ribeiro, Prevention of zeolite deactivation by coking, J. Mol. Catal. A Chem. 305 (2009) 69–83.
- [31] M. Choi, K. Na, J. Kim, Y. Sakamoto, O. Terasaki, R. Ryoo, Stable single-unit-cell nanosheets of zeolite MFI as active and long-lived catalysts (vol 461, pg 246, 2009), Nature 461 (2009) 1.
- [32] L. Zhao, B. Shen, J. Gao, C. Xu, Investigation on the mechanism of diffusion in mesopore structured ZSM-5 and improved heavy oil conversion, J. Catal. 258 (2008) 228–234.
- [33] M.B. Gao, H. Li, M. Yang, J.B. Zhou, X.S. Yuan, P. Tian, M. Ye, Z.M. Liu, A modeling study on reaction and diffusion in MTO process over SAPO-34 zeolites, Chem. Eng. J. 377 (2019) 12.